

COMMUNICATION

On-chip development of hydrogel microfibers from round to square/ribbon shape†

Cite this: *J. Mater. Chem. A*, 2014, 2, 4878

Zhenhua Bai,^a Janet M. Mendoza Reyes,^b Reza Montazami^a and Nastaran Hashemi^{*a}

Received 7th November 2013
Accepted 20th January 2014

DOI: 10.1039/c3ta14573e

www.rsc.org/MaterialsA

We use a microfluidic approach to fabricate gelatin fibers with controlled sizes and cross-sections. Uniform gelatin microfibers with various morphologies and cross-sections (round and square) are fabricated by increasing the gelatin concentration of the core solution from 8% to 12%. Moreover, the increase of gelatin concentration greatly improves the mechanical properties of gelatin fibers; the Young's modulus and tensile stress at break of gelatin (12%) fibers are raised about 2.2 and 1.9 times as those of gelatin (8%) fibers. The COMSOL simulations indicate that the sizes and cross-sections of the gelatin fibers can be tuned by using a microfluidic device with four-chevron grooves. The experimental results demonstrate that the decrease of the sheath-to-core flow-rate ratio from 150 : 1 to 30 : 1 can increase the aspect ratio and size of ribbon-shaped fibers from 35 μm \times 60 μm to 47 μm \times 282 μm , which is consistent with the simulation results. The increased size and shape evolution of the cross-section can not only strengthen the Young's modulus and tensile stress at break, but also significantly enhance the tensile strain at break.

The development of biocompatible polymeric fibers has received a lot of attention due to their outstanding physical and chemical properties.^{1,2} Among the various materials, gelatin is an inexpensive, neutral, water-soluble, non-toxic, and FDA-approved biopolymer with excellent biocompatibility, biodegradability, and cell adhesiveness, which is extensively used in medical products, such as wound dressings, drug delivery systems, and tissue engineering.^{3–12} Until now, gelatin has been fabricated in various forms, *e.g.*, films,¹³ nanoparticles,¹⁴ and porous hydrogels.¹⁵ There are several studies to produce functional gelatin fibers by electrospinning, because of the high surface area, high porosity, and flexibility for surface functionalization of gelatin based fibers.^{3–5} Various solvent systems have been used to prepare electrospinnable gelatin solutions, such as

2,2,2-trifluoroethanol (TFE), formic acid, 1,1,1,3,3,3-hexafluoro-2-propanol (HFP), and acetic acid.^{7,9} The diameters of the previously obtained electro-spun gelatin fibers were in the range of 100–1900 nm, and there is no report on microfibers with larger diameters using the electrospinning method.¹⁰ Furthermore, the cross-sectional shape of electro-spun fibers is almost exclusively limited to round shape due to interfacial tension between the solvent/fiber material solution and air.¹² Although there have been some reports on fabrication of gelatin fibers with relatively larger size by gel-spinning, the obtained fibers are less-uniform, and this method does not allow for tuning of the cross-section and size.^{4,16} It is well known that fibers with complex shapes have improved mechanical properties and larger surface area, and are promising materials for biological microreactors, tissue engineering, and controlled release.¹⁷ Therefore, the development of a novel method to fabricate gelatin fibers with controlled sizes and shapes is highly demanded.

Recently, a microfluidic device based fabrication method has been recognized as an efficient method for the fabrication of micron-sized fibers due to its low-material consumption, conventional volume and size control, enhanced reaction rate, and inexpensive tooling costs.^{18–22} Compared with other fiber fabrication methods, the microfluidic method has a unique advantage that can create fibers with a range of cross-sectional shapes.^{18,23} The shape of the fiber is influenced by the flow rates and the types and numbers of shaping elements in the channel walls, such as various grooves.¹⁶ At present, great efforts have been devoted to expand the variety of materials and types of structures which can be successfully fabricated by microfluidic devices.¹⁷ For instance, Thangawng *et al.* produced round PMMA fibers with diameters down to 300 nm by varying the ratio between the sheath and core flow rates using a 5-diagonal groove device, and ribbon-shaped fibers with submicron thickness were also fabricated using a 7-chevron/5-diagonal groove combination device.²³ Moreover, Boyd *et al.* succeeded in fabricating “double anchor” shaped thiol-end fibers using a two-stage hydrodynamic focusing system.²⁴ However, to the best

^aDepartment of Mechanical Engineering, Iowa State University, Ames, IA 50011, USA. E-mail: nastaran@iastate.edu

^bDepartment of Computer Engineering, University of Puerto Rico, 00681, Puerto Rico

† Electronic supplementary information (ESI) available. See DOI: 10.1039/c3ta14573e

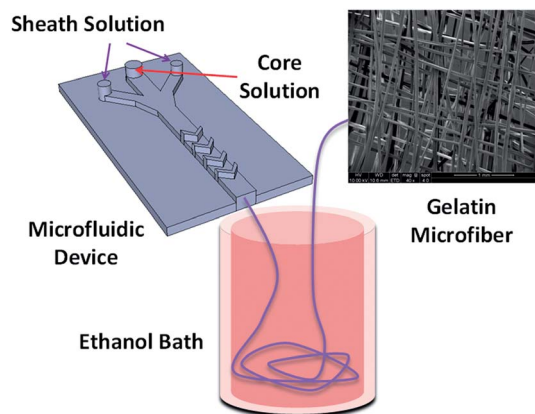


Fig. 1 Schematic illustration of the experimental setup for gelatin fiber fabrication, and the SEM image of gelatin microfibers fabricated by 11% gelatin concentrations at the sheath and core flow-rates of 1500 and $10 \mu\text{L min}^{-1}$, respectively.

of our knowledge, there still has been no study on fabrication of biocompatible gelatin fibers by the microfluidic method.

In the present work, we fabricate gelatin fibers using a microfluidic approach for the first time. Using surface patterns (grooves) on the top and bottom of a microchannel, we hydrodynamically focus the prepolymer stream at the center of the microchannel to create microfibers with specific shapes and sizes. The approach is to simultaneously exploit the properties of the hydrogel and laminar flow to control the cross-sectional shape and size during the polymerization process. The grooves generate hydrodynamic lift resulting in the sheath fluid to vertically move the prepolymer stream towards the center of the channel.^{25–27} The prepolymer shape will be locked in by coming into contact with the sheath flow. We systematically increase the gelatin concentration in DMSO solvent to investigate the effect of the viscosity of core solution on the morphology, cross-section and mechanical properties of gelatin fibers. The COM-SOL simulations indicate that the cross-section of gelatin fibers

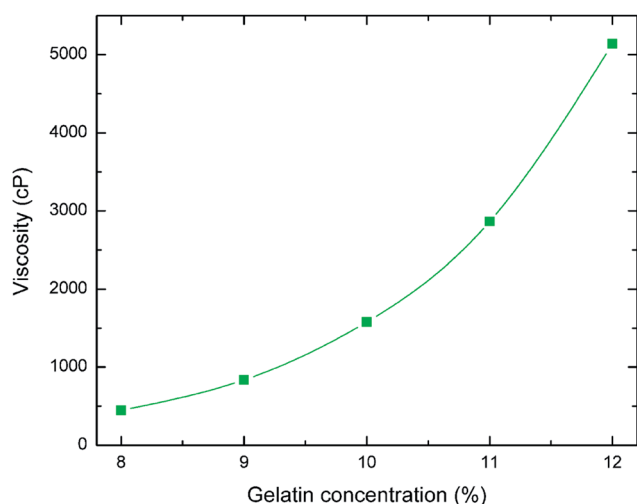


Fig. 2 Viscosity of core solutions prepared by various gelatin concentrations in DMSO solution.

can be tuned by using a microfluidic device with four-chevron grooves. The experimental results demonstrate that the decrease of sheath-to-core flow-rate ratio results in the increase of fiber dimensions from $30 \mu\text{m} \times 30 \mu\text{m}$ to $47 \mu\text{m} \times 282 \mu\text{m}$, which complies with the simulation results. The mechanical characterization (Young's modulus, tensile stress at break, and tensile strain at break) indicates that both the gelatin concentration and cross-section can influence the mechanical performance of gelatin fibers.

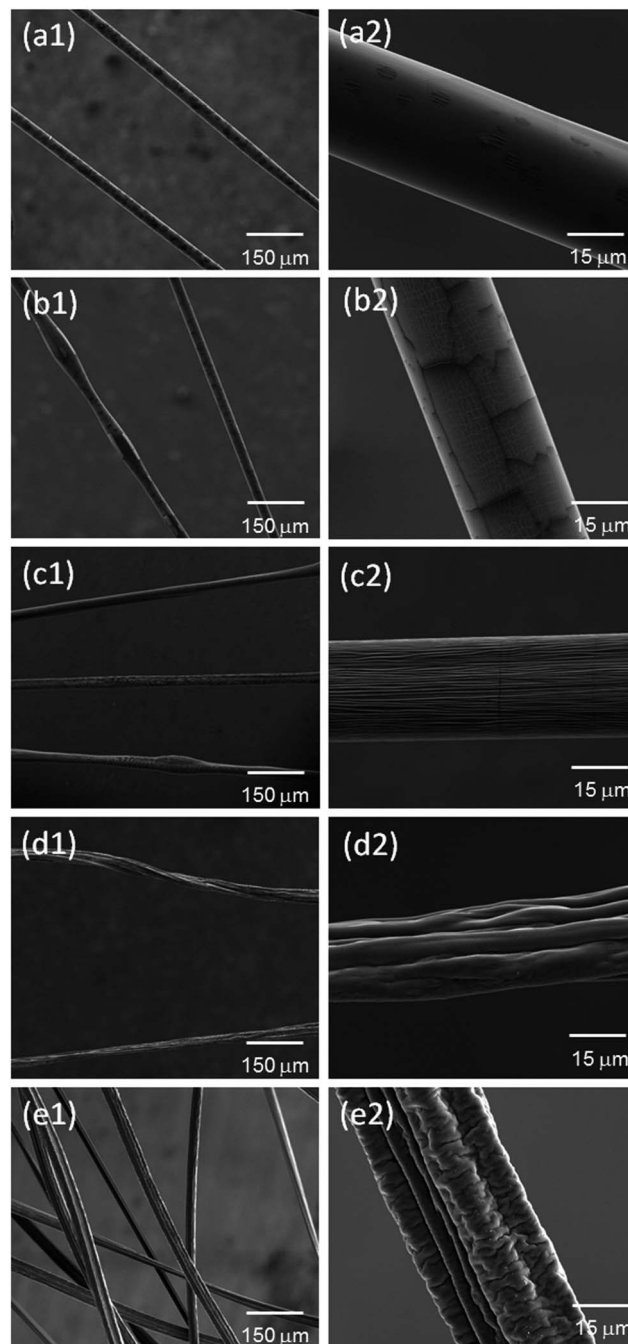


Fig. 3 SEM images of gelatin microfibers fabricated by gelatin concentrations of (a) 8%, (b) 9%, (c) 10%, (d) 11%, and (e) 12% in DMSO solution. The sheath and core flow-rates are set as 1500 and $5 \mu\text{L min}^{-1}$, respectively.

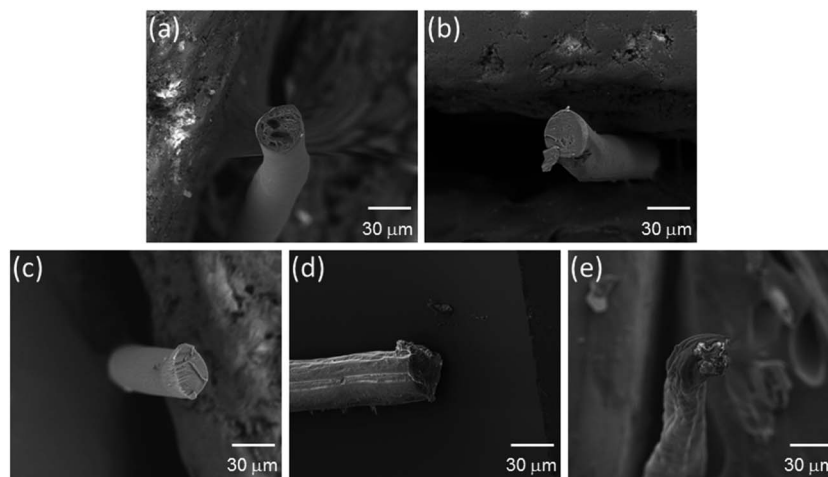


Fig. 4 Cross-sectional SEM images of gelatin microfibers fabricated by gelatin concentrations of (a) 8%, (b) 9%, (c) 10%, (d) 11%, and (e) 12% in DMSO solution. The sheath and core flow-rates are set as 1500 and 5 $\mu\text{L min}^{-1}$, respectively.

Fig. 1 illustrates the production method for gelatin microfibers utilizing a microfluidic device. The fluids were driven by syringe pumps using silicone tubing before entering the channel. The channel consists of three inlets, a single, central core fluid inlet and two inlets for the sheath fluid (Fig. S1†). At the junction of the three inlets, hydrodynamic focusing takes place, which compresses the core into a thin vertical strip which spans the height of the channel. At the same time, the gelatin stream rapidly dries upon contact with an ethanol bath and turns into a cluster of microfibers since ethanol is a miscible agent to DMSO but an anti-solvent to gelatin. Downstream from the focusing region, a series of four chevron-shaped grooves are incorporated into the ceiling and floor of the channel which induce compression of gelatin fibers perpendicular to the main flow direction. The grooves are designed to compress the core fluid vertically into a desired cross-sectional shape. As the polymerized fiber exits the channel, the fibers are collected in an ethanol bath and then rolled up into a copper holder for characterization (Fig. S2†). The SEM image in Fig. 1 shows the gelatin microfibers fabricated by 11% gelatin concentrations at the sheath and core flow-rates of 1500 and 10 $\mu\text{L min}^{-1}$, respectively.

To highlight the versatility of this fabrication process, we generated fibers using core solutions with various gelatin concentrations in DMSO solvent. As shown in Fig. 2, the viscosity of the core solution significantly increases from 446 to 5140 cP, when the gelatin concentration increases from 8% to 12%. It is noted that the increase of gelatin concentration by 1% results in the increase of viscosity by 1.8 times on average. Fig. 3 shows the field emission scanning electron microscopy (FE-SEM) images of representative fibers obtained at different gelatin concentrations. The sheath and core flow-rates are set as 1500 and 5 $\mu\text{L min}^{-1}$, respectively. It can be seen that all fibers are very uniform with a width about 30 μm , which proves that the microfluidic method is useful in a large viscosity range. Interestingly, the gelatin concentration shows a significant effect on the morphology of fibers. The gelatin (8%) fiber shows

a very smooth surface with a series of black spots. When the gelatin concentration increases to 9%, the surface shows many cracked patterns. When the gelatin concentration exceeds 10%, full of lines are observed on the fiber surface, and the lines become larger by the increase of gelatin concentration. The cross-sections of the above gelatin fibers are also shown in Fig. 4. It is revealed that round-shaped cross-sections are obtained in a lower gelatin concentration range (8–10%), and the shape evolution from round to square is confirmed by the further increase of gelatin concentration (11–12%). The above results reveal the surface variation from smooth to rough and shape evolution from round to square by the increase of gelatin concentration.

The formation process of fibers can be explained as follows: first, the DMSO solution can be dissolved in ethanol by the mixing of core and sheath solution. Then, the gelatin is condensed into a fiber structure due to its indissolubility in ethanol. In this process, the viscosity of the gelatin solution plays an important role in the formation of the fiber surface. The condensation of dense gelatin results in rough connection between gelatin pieces, which is favorable to obtain complicated morphologies and shapes. Li *et al.* have investigated the effect of gelatin concentration on gelatin fibers using the electrospinning method, and they reported that the decrease in fiber diameter from ~ 500 to ~ 200 nm occurs when the initial gelatin concentration in HFP is reduced from 8.3% to 5%.²⁸ Choktaweasap *et al.* dissolved gelatin in glacial acetic acid to synthesize gelatin fibers by electrospinning, and found that the fiber diameter increases from 214 nm to 839 nm with the increase of gelatin concentration from 15% to 29%.³ However, such a phenomenon has not been observed in our work, where the fiber size has no relationship with gelatin concentration in DMSO. It is also reported that the fabrication of pure gelatin fibers is difficult by electrospinning, which is commonly accompanied by a significant formation of beads, especially in a low gelatin concentration regime.^{3,28,29} By using the microfluidic approach, one can effectively eliminate the formation of any

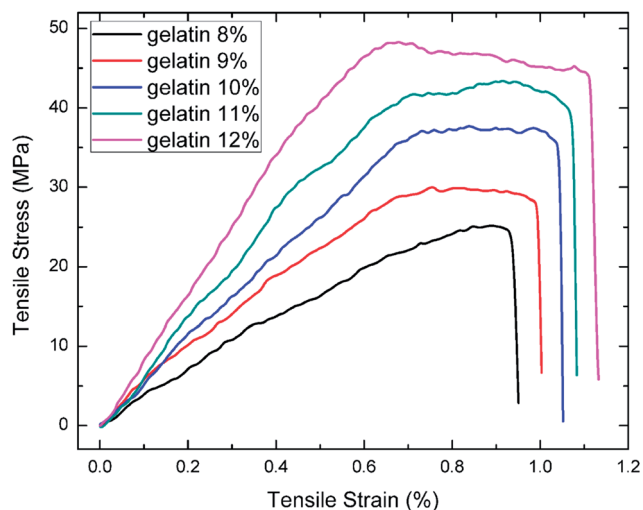


Fig. 5 Tensile stress–tensile strain curves of gelatin fibers with different gelatin concentrations in DMSO solution. The sheath and core flow-rates are set as 1500 and $5 \mu\text{L min}^{-1}$, respectively.

by-product, and uniform gelatin fibers can be produced as long as we want. The present result is the first observation of such a morphology and cross-section change of gelatin fibers, which has not been realized by other methods. It should be mentioned that the formed line structures can effectively increase the surface area of gelatin fibers, which is beneficial for applications in tissue engineering and drug delivery.¹⁹

The tensile stress–tensile strain curves of gelatin fibers fabricated by different gelatin concentrations are shown in Fig. 5. Table 1 summarizes the values of Young's modulus, tensile stress at break, and tensile strain at break of all samples. It can be seen that the increase of gelatin concentration greatly improves the mechanical properties of gelatin fibers. The gelatin (8%) fiber exhibits a Young's modulus of 3750 MPa and a tensile stress at break of 25.2 MPa. When the gelatin concentration reaches 12%, the Young's modulus and tensile stress at break are raised to 8366 and 48.4 MPa, which are 2.2 and 1.9 times those of gelatin (8%) fibers. On the other hand, the tensile strain at break shows little dependence on gelatin concentration, which is slightly increased from 0.95% to 1.13%. Fukae *et al.* have reported that the gelatin fiber, which is fabricated by extrusion of 15 wt% gelatin in DMSO into methanol at -20°C , exhibits a Young's modulus of 2300 MPa and a tensile stress at

Table 1 Mechanical properties of gelatin fibers with different gelatin concentrations in DMSO solution. The sheath and core flow-rates are set as 1500 and $5 \mu\text{L min}^{-1}$, respectively

Sample	Young's modulus (MPa)	Tensile stress at break (MPa)	Tensile strain at break (%)
Gelatin 8%	3750	25.2	0.95
Gelatin 9%	4418	30.1	0.99
Gelatin 10%	5253	37.7	1.05
Gelatin 11%	6687	43.5	1.08
Gelatin 12%	8366	48.4	1.13

break of 146 MPa.⁴ According to previous publications, the achieved Young's modulus in our work is the highest compared with any other fabrication method.^{16,29–31} The moderate tensile stress at break is due to the relatively low tensile strain at break. Though higher gelatin concentration is favorable for better mechanical properties, it is difficult to further increase the gelatin concentration in the present experiment because of the occurrence of channel blocking by highly viscous gelatin solution.

Fig. 6a presents the concentration profile slices of core and sheath solutions (1 : 150) in the whole channel. Initially, the core solution is sandwiched vertically between two sheath streams. During passing chevron grooves, the sheath fluid moves from the sides of the channel to the top and bottom of the channel, confining the core stream to the center line of the channel and simultaneously dictating the core fluid's cross-sectional shape. As with the output channel alignment, polymerization downstream of the shaping region preserves this cross-sectional shape. The simulation results reveal the effect of sequential chevrons driving the flow from a thin vertical strip into a ribbon-shaped flow prior to polymerization. Fig. 6b–d

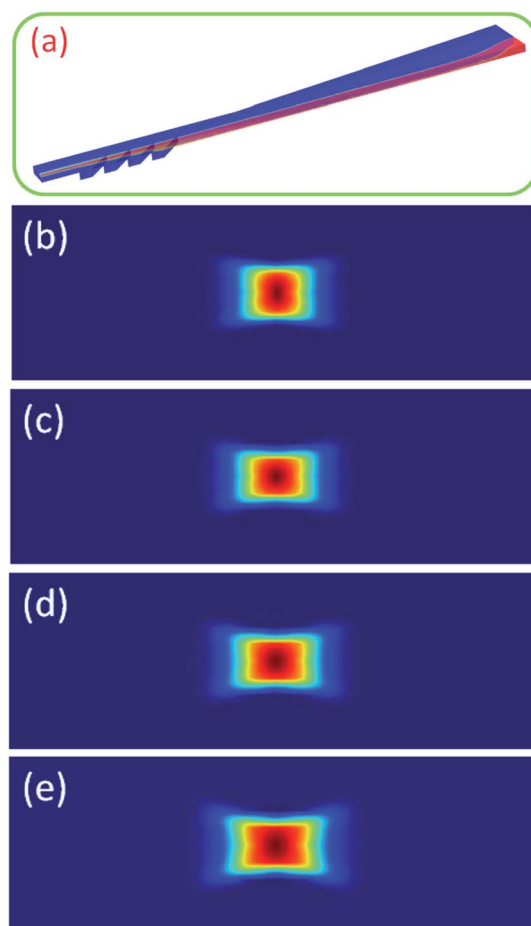


Fig. 6 (a) Illustration of concentration profile slices of sheath and core solutions (150 : 1) in the YZ plane, beginning after the core has been focused and then after four chevrons. The simulated cross-sections at the sheath-to-core flow-rate ratios of (b) 300 : 1, (c) 150 : 1, (d) 75 : 1, and (e) 30 : 1. The sample stream is red and the sheath fluid is blue.

give the simulated cross-sections for sheath-to-core flow-rate ratios ranging from 300 : 1 to 30 : 1 in our microfluidic device. It reveals that the cross-section of gelatin fibers has a tendency from square to ribbon as the flow-rate ratio between the sheath and core solutions decreases.

The comparison of cross-sectional shapes of gelatin fibers fabricated using various gelatin concentrations and simulation results obtained at the sheath-to-core flow-rate ratio of 300 : 1 indicates that the high gelatin concentration samples (10–11%) are consistent with the simulation results. In order to test whether the simulation results are suitable for lower sheath-to-core flow-rate ratio samples or not, the gelatin (9%) fibers are fabricated by decreasing the sheath-to-core flow-rate ratio in a large range. Fig. 7a–c show the cross-sections of gelatin (9%) fibers fabricated by varying the flow-rate ratio between the sheath and the core from 150 : 1 to 30 : 1. As is shown, the decrease of the sheath-to-core flow-rate ratio can not only increase the aspect ratio of fibers, but also increase the fiber size. The dimensions of the fibers are plotted in Fig. 7d. Fibers

with dimensions (height \times width) from $30\ \mu\text{m} \times 30\ \mu\text{m}$ to $47\ \mu\text{m} \times 282\ \mu\text{m}$ were successfully fabricated. As is evident from these images, the actual cross-sectional shapes of the gelatin fibers obtained were in general agreement with those of the COMSOL simulations (Fig. 6), in terms of the shape evolution for those fibers obtained at various flow-rates. It should be mentioned that the further increase of fiber dimensions is restricted by the channel size, which easily causes clogging before the outlet. However, the gelatin fibers with more complicated shapes should be possible to fabricate by introducing different groove types and changing the channel size of the microfluidic device.

For the purpose of studying the effect of cross-section on the mechanical performance, the mechanical properties of gelatin fibers fabricated by different sheath-to-core flow-rate ratios are compared in Fig. 8. It is revealed that the mechanical performances of gelatin (8–10%) fibers are significantly influenced by the variation of the flow-rate ratio. With the decrease of flow-rate ratio between the sheath and the core from 300 : 1 to 75 : 1, the Young's modulus, tensile stress at break, and tensile strain

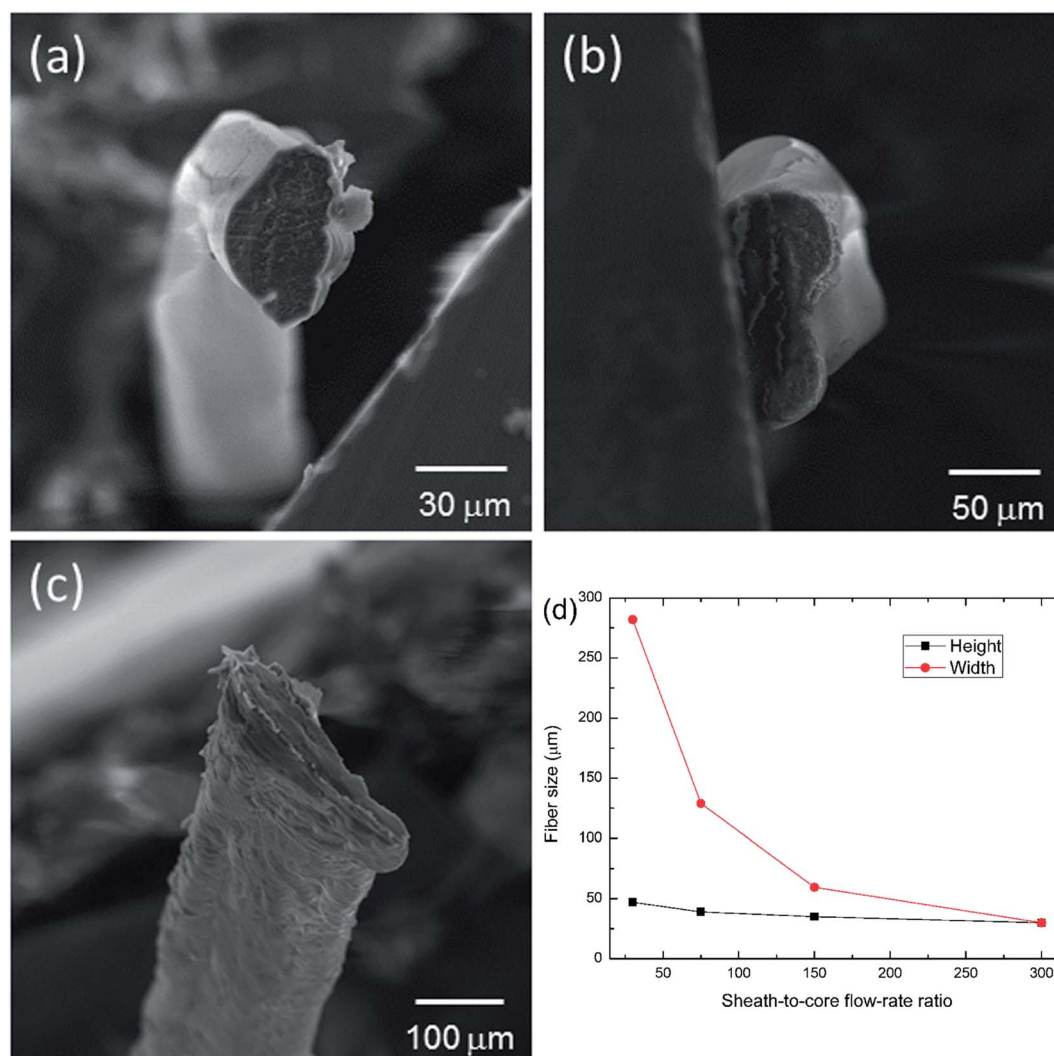


Fig. 7 SEM images of gelatin (9%) microfibers fabricated by sheath-to-core flow-rate ratios of (a) 150 : 1, (b) 75 : 1, and (c) 30 : 1. (d) Cross-sectional dimensions of the gelatin fibers as a function of the sheath-to-core flow-rate ratios in the microfluidic device.

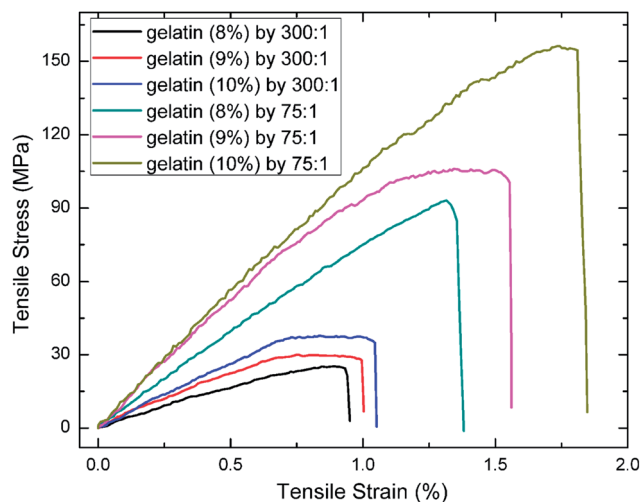


Fig. 8 Tensile stress–tensile strain curves of gelatin (8–10%) fibers fabricated by sheath-to-core flow-rate ratios of 300 : 1 and 75 : 1, respectively.

at break of gelatin (9%) fibers are strongly enhanced by 2.3, 3.5, and 1.6 times, respectively. Particularly, the enhancements of tensile strain at break for gelatin 8%, 9% and 10% fibers reach 1.46, 1.6, and 1.84 times, respectively. Our results clearly indicate that the increased size and shape evolution can not only strengthen the Young's modulus and tensile stress at break, but also significantly enhance the tensile strain at break. It is believed that the combination effect of increased size and ribbon cross-section should be responsible for the enhanced mechanical performance. Therefore, by adjusting the gelatin concentration in core solution and the sheath-to-core flow-rate ratio, the mechanical properties of gelatin fibers can be well controlled for application in tissue engineering scaffolds, which can be used for engineering load-bearing tissues such as bone or cartilage.¹¹

In summary, gelatin fibers with controlled size and shape are fabricated by using a microfluidic device using gelatin dissolved DMSO solution as the core solution and ethanol as the sheath solution. The viscosity of the core solution increases from 446 to 5140 cP by the increase of gelatin concentration from 8% to 12%, which significantly changes the fiber morphology from smooth to rough and the cross-section from round to square. Moreover, the mechanical properties of gelatin fibers are significantly improved by the increase of gelatin concentration, the Young's modulus and tensile stress at break of gelatin (12%) fibers are raised about 2.2 and 1.9 times those of gelatin (8%) fibers. On the other hand, with the decrease of flow-rate ratio between the sheath and the core from 150 : 1 to 30 : 1, ribbon-shaped gelatin fibers can be obtained, and the fiber dimensions (height × width) remarkably increase from 35 μm × 60 μm to 47 μm × 282 μm. The experimental results fit well with the simulation results in terms of shape evolution. The novel cross-sections of gelatin fibers are beneficial to enhance the Young's modulus, tensile stress at break, and tensile strain at break.

Acknowledgements

We gratefully acknowledge the Iowa State University Health Research Initiative (ISU-HRI) and the William March Scholar program for support of this work. The authors would like to thank Mahendra Thunga for help with the measurements of mechanical properties.

References

- 1 M. A. Daniele, S. H. North, J. Naciri, P. B. Howell, S. H. Foulger, F. S. Ligler and A. A. Adams, *Adv. Funct. Mater.*, 2013, **23**, 698–704.
- 2 D. Zaytseva-Zotova, V. Balyshva, A. Tsoy, M. Drozdova, T. Akopova, L. Vladimirov, I. Chevalot, A. Marc, J. L. Goergen and E. Markvicheva, *Adv. Eng. Mater.*, 2011, **13**, B493–B500.
- 3 N. Choktaweasap, K. Arayanarakul, D. Aht-Ong, C. Meechaisue and P. Supaphol, *Polym. J.*, 2007, **39**, 622–631.
- 4 R. Fukae and T. Midorikawa, *J. Appl. Polym. Sci.*, 2008, **110**, 4011–4015.
- 5 P. Sikareepaisan, A. Suksamrarn and P. Supaphol, *Nanotechnology*, 2008, **19**, 015102.
- 6 S. E. Kim, D. N. Heo, J. B. Lee, J. R. Kim, S. H. Park, S. Jeon and I. K. Kwon, *Biomed. Mater.*, 2009, **4**, 044106.
- 7 J. Ratanavaraporn, R. Rangkupan, H. Jeeratawatchai, S. Kanokpanont and S. Damrongsakkul, *Int. J. Biol. Macromol.*, 2010, **47**, 431–438.
- 8 S. Suganya, T. S. Ram, B. S. Lakshmi and V. R. Giridev, *J. Appl. Polym. Sci.*, 2011, **121**, 2893–2899.
- 9 D. Sahoo and P. L. Nayak, *Int. J. Mater. Res.*, 2012, **103**, 1395–1399.
- 10 B. S. Chiou, H. Jafri, R. Avena-Bustillos, K. S. Gregorski, P. J. Bechtel, S. H. Imam, G. M. Glenn and W. J. Orts, *Int. J. Biol. Macromol.*, 2013, **55**, 214–220.
- 11 L. H. Han, S. Yu, T. Y. Wang, A. W. Behn and F. Yang, *Adv. Funct. Mater.*, 2013, **23**, 346–358.
- 12 C. D. Mu, X. Y. Li, J. M. Guo, C. X. Bi and D. F. Li, *J. Appl. Polym. Sci.*, 2013, **129**, 773–778.
- 13 A. Jongjareonrak, S. Benjakul, W. Visessanguan, T. Prodpran and M. Tanaka, *Food Hydrocolloids*, 2006, **20**, 492–501.
- 14 J. Vandervoort and A. Ludwig, *Eur. J. Pharm. Biopharm.*, 2004, **57**, 251–261.
- 15 Y. Tabata, S. Hijikata and Y. Ikada, *J. Controlled Release*, 1994, **31**, 189–199.
- 16 R. Fukae, A. Maekawa and S. Sangen, *Polymer*, 2005, **46**, 11193–11194.
- 17 A. R. Shields, C. M. Spillmann, J. Naciri, P. B. Howell, A. L. Thangawng and F. S. Ligler, *Soft Matter*, 2012, **8**, 6656–6660.
- 18 A. L. Thangawng, P. B. Howell, J. J. Richards, J. S. Erickson and F. S. Ligler, *Lab Chip*, 2009, **9**, 3126–3130.
- 19 D. A. Boyd, A. R. Shields, J. Naciri and F. S. Ligler, *ACS Appl. Mater. Interfaces*, 2013, **5**, 114–119.
- 20 A. Duboin, R. Middleton, F. Malloggi, F. Monti and P. Tabeling, *Soft Matter*, 2013, **9**, 3041–3049.

- 21 A. Karimi, S. Yazdi and A. M. Ardekani, *Biomicrofluidics*, 2013, **7**, 021501.
- 22 J. K. Nunes, H. Constantin and H. A. Stone, *Soft Matter*, 2013, **9**, 4227–4235.
- 23 A. L. Thangawng, P. B. Howell, C. M. Spillmann, J. Naciri and F. S. Ligler, *Lab Chip*, 2011, **11**, 1157–1160.
- 24 D. A. Boyd, A. R. Shields, P. B. Howell and F. S. Ligler, *Lab Chip*, 2013, **13**, 3105–3110.
- 25 N. Hashemi, J. S. Erickson, J. P. Golden, K. M. Jackson and F. S. Ligler, *Biosens. Bioelectron.*, 2011, **26**, 4263–4269.
- 26 N. Hashemi, J. S. Erickson, J. P. Golden and F. S. Ligler, *Biomicrofluidics*, 2011, **5**, 032009.
- 27 N. Hashemi, P. B. Howell, J. S. Erickson, J. P. Golden and F. S. Ligler, *Lab Chip*, 2010, **10**, 1952–1959.
- 28 M. Y. Li, M. J. Mondrinos, M. R. Gandhi, F. K. Ko, A. S. Weiss and P. I. Lelkes, *Biomaterials*, 2005, **26**, 5999–6008.
- 29 Z. M. Huang, Y. Z. Zhang, S. Ramakrishna and C. T. Lim, *Polymer*, 2004, **45**, 5361–5368.
- 30 M. Y. Li, Y. Guo, Y. Wei, A. G. MacDiarmid and P. I. Lelkes, *Biomaterials*, 2006, **27**, 2705–2715.
- 31 P. O. Rujitanaroj, N. Pimpha and P. Supaphol, *Polymer*, 2008, **49**, 4723–4732.